3 Devices

3-1 Oscillator

3-1-1 GaAs-based Quantum Cascade Lasers

SEKINE Norihiko and HOSAKO Iwao

Quantum cascade lasers (QCLs) have different structures and characteristics from those of conventional semiconductor lasers commonly used in the optical communication systems. Therefore, QCLs make it possible for us to access wavelengths which couldn't be available in conventional lasers. In particular, terahertz QCLs (THz-QCLs) have been paid much attention due to their potential applications in various fields, such as biosensing, imaging, and security. In this paper, we report GaAs-based THz-QCLs. The peak output power of about 30 mW was obtained in a pulsed operation at low temperature. The maximum operating temperature above 120 K was achieved.

Keywords
Terahertz, Quantum cascade laser, Intersubband transition

1 Introduction — What is a quantum cascade laser (QCL)?

A quantum cascade laser (QCL) is a type of laser with structures, emission mechanisms, and characteristics that differ significantly from those of conventional semiconductor lasers commonly used in optical communication systems and compact disc players. Figure 1 (a) shows the energy band profile of a conventional semiconductor laser. The figure shows the example of a quantum well (QW) laser that uses semiconductor quantum wells in the active layer. In this device one or several QW active layers are sandwiched between n-doped and p-doped semiconductors. On the other hand, Fig. 1 (b) shows the typical energy band profile of a QCL. A QCL consists of nanometer-order layers of semiconductor materials having different energy barriers. At a glance, structures may appear similar as they both contain layers of several types of semiconductor materials. However, the mechanisms of operation and relative performance of these different structures diverge dramatically. Let us compare a QCL with a conventional semiconductor laser (referred simply to as a "semiconductor laser" below).

A semiconductor laser emits light as a result of a phenomenon known as interband transition, which is the radiative recombination of the electrons in the conduction band of the semiconductor and the holes in the valence band of the semiconductor [Fig. 1 (a)]. For this reason, the emission wavelength depends on the band gap energy, E_g (plus the quantization energy in the case of a QW laser) of the semiconductor material used in the active layer. On the other hand, a QCL uses only the electrons in the conduction band (or the holes in the valence band), as shown in Fig. 1 (b), and emits light as a result of the intersubband

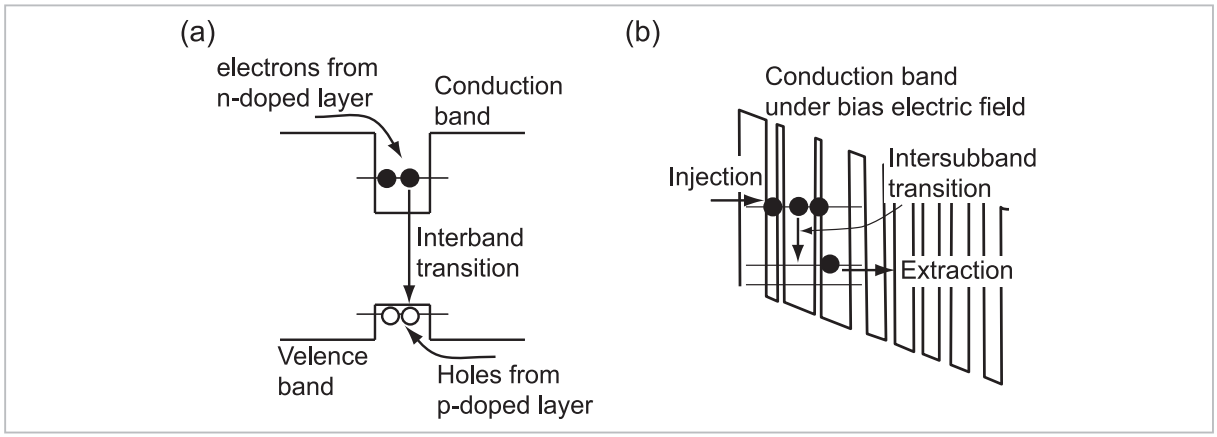

Fig.1 *Energy band profile in active layer*

(a) A conventional semiconductor laser emits light as a result of electron-hole interband transition.
(b) A quantum cascade laser (QCL) emits light as a result of intersubband transition.

transition between the quantized states that appear when the quantum wells are fabricated. For this reason, when a QCL is discussed, the semiconductor laser is often referred to as an interband transition laser or a bipolar laser, and the QCL as the intersubband transition laser or the unipolar laser, to clearly distinguish between the two types of lasers.

Due to these differences, a QCL has the features listed below, as compared to a semiconductor laser.

(1) Freely designed emission wavelengths

A QCL emits light as a result of intersubband transition, such that its emission wavelength is determined by the energy difference between the subbands. The energy difference between these subbands can be arbitrarily controlled by the width of the quantum wells. This means that the emission wavelength is not restricted by the component materials.

(2) Significant quantum efficiency

As shown in Fig. 2 (a), the active layer of a QCL features a multistage structure connecting many units, each of which consists of a gain region (which emits light as a result of the intersubband transition between the upper and lower states of the laser) and a carrier extraction/injection region (which hands over the carriers relaxed to the lower state of the laser to the next unit). As a result, a QCL exhibits the carrier recycling effect, in which a carrier that has been subject to radiative transition moves to the next unit and becomes involved in another radiative transition process. Consequently, significant quantum efficiency can be obtained, in proportion to the number of units connected. Figure 2 (b) shows a schematic diagram of the process by which a carrier undergoes transitions between states, from higher potential energy to lower potential energy. Since this carrier behavior can be pictured as a fall through levels of potential energy (i.e., a cascade) during radiative transitions, this laser is referred to as a quantum cascade laser, or QCL.

(3) High optical gain and narrow optical gain width

We have stated that a QCL emits light as a result of intersubband transition while a semiconductor laser emits light as a result of interband transition. A significant difference arises from this difference in the transition mechanism. Figure 1 shows the energy band profiles in the direction perpendicular to the plane of the quantum wells. Figure 3 focuses on the upper and lower states of the laser and shows the energy dispersion relationships in the direction parallel to the plane. For comparison, we will first discuss the semiconductor laser. As shown in Fig. 3 (b), the curvatures of the dispersion curves feature opposite signs for the conduction band (filled with electrons) and the valence band (filled with holes). As a radiative transition is a vertical transition, the

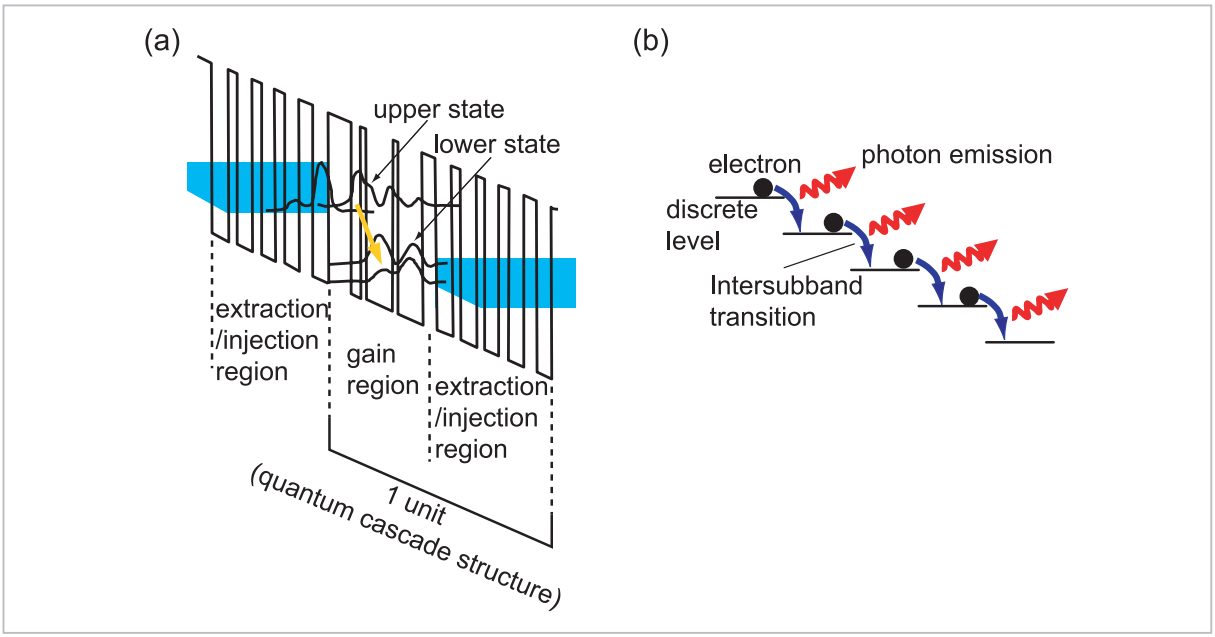

Fig.2 *(a) Example of QCL active layer construction. A gain region and a carrier extraction/injection region constitute a unit (QC structure).*
(b) Schematic diagram of carrier dynamics in the active layer connecting many stages of QC structures.

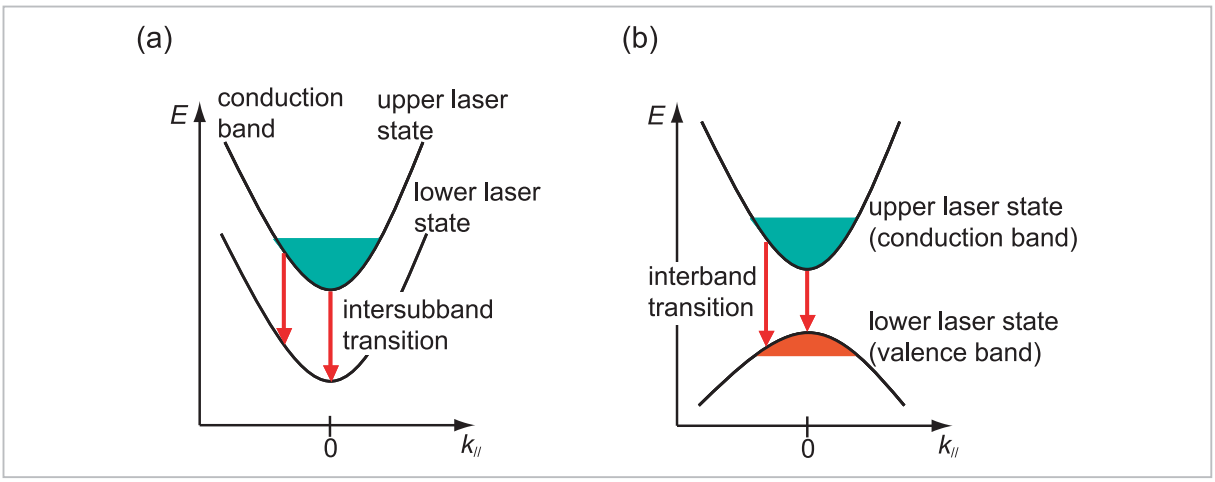

Fig.3 *Energy dispersion curves parallel to quantum well (QW) plane in gain region*

(a) For a QCL, the transition energy is approximately constant independent of $k_{//}$.

(b) For a semiconductor laser, the transition energy increases as $k_{//}$ increases.

transition energy at k = 0 ($E_{k=0}$) and that at $k \neq 0$ ($E_{k\neq 0}$) differ. As the transition energy depends on k in this manner, the joint density of states also has an energy width, and the gain spectrum is described by a step function. On the other hand, as shown in Fig. 3 (a), in the case of a QCL, the dispersion curves of the two states are both within either the conduction or the valence band, such that both display the same curvature. If we then ignore the non-parabolic nature of the dispersion curves, Ek is constant, independent of k (= E). Consequently, the joint density of states has a non-zero value only near the transition energy, and the gain spectrum is described by a delta function, which is characteristic of an atomic state. For this reason, all of the injected carriers are used in the transition of energy E in the light emission process, and this characteristic consequently produces a high optical gain. We

can also expect a narrow line width due to the essential characteristic of a QCL: the gain spectrum is described by a delta function.

In 1971, Kazarinov and Suris proposed a laser structure that can be considered the prototype of a QCL. This proposal pointed to the possibility of optical amplification based on intersubband transition[1]. This proposal increased active theoretical and experimental research into intersubband transition in terms of both basic research and applications[2]-[9]. Through these research activities, the method of current injection and the generation of population inversion became the focus of particular discussion. Finally, in 1994, Faist et al. succeeded in the first QCL oscillation with an intersubband laser operating in the mid-infrared (MIR) range[10]. Following this successful laser oscillation, diverse techniques were devised to improve laser performance. Today, continuous room-temperature operation and watt-class output are now possible. However, in the terahertz (THz) band, the emission energy is far smaller than in the MIR range, leading to various difficulties particular to the THz band. Nevertheless, in 2002, Köhler et al. succeeded in developing a QCL in the THz band (THz-QCL)[11].

The sections below describe the activities of NICT related to the THz-QCL and introduce the characteristics that have been identified to date.

2 Terahertz (THz) quantum cascade laser (QCL)

2.1 Principle of operation

Several well-known structures have been adopted in the THz-QCL. Figure 4 shows one of these structures. We have already stated that the unit forming the active layer consists of a gain region and a carrier extraction/injection region. More specifically, the gain region contains the upper state (3) and the lower state (2) of the laser for producing the light emission, and the energy difference, E_{32}, determines the oscillation frequency. We need to inject carriers (in this case, electrons) to state 3. This

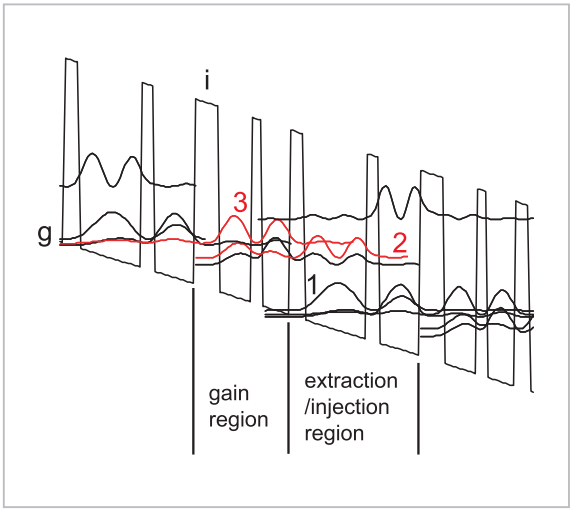

Fig.4 *Example energy band diagram for the THz-QCL*

Here, "i" indicates the injection barrier, and "g" indicates the ground state of the carrier extraction/injection region. "3" and "2" indicate the upper and lower states of the laser, respectively. "1" indicates the carrier extraction state attained using LO phonons.

injection is achieved as the electrons in the minimum energy level (g) in the carrier extraction/injection region of the previous stage tunnel through a thin film with controlled thickness, referred to as the injection barrier (the semiconductor layer indicated by "i" in the figure). To produce the laser oscillation, a population inversion needs to be generated between states 3 and 2. The rate expressions for the carrier number and the photon number are expressed below, in a manner similar to that seen in the semiconductor laser.

$$\frac{dn_3}{dt} = \frac{J}{e} - \frac{n_3}{\tau_3} - Sg(n_3 - n_2) \quad (1)$$

$$\frac{dn_2}{dt} = \frac{n_3}{\tau_{32}} + Sg(n_3 - n_2) - \frac{n_2 - n_g \exp(-\Delta/kT)}{\tau_2} \quad (2)$$

$$\frac{dS}{dt} = \left(\frac{c}{N}\right)\left\{S\left[g(n_3 - n_2) - \alpha\right] + \beta\frac{n_3}{\tau_{sp}}\right\} \quad (3)$$

Here, n_i is the carrier density of state i, τ_i is the carrier lifetime of state i, J is the current density, e is the elementary charge, S is the photon density, g is the gain coefficient, τ_{ij} is

the carrier transition time from state i to state j, Δ is the energy difference between states 2 and 1, kT is the thermal energy, c is the speed of light, N is the equivalent refractive index of the QCL waveguide, α is the absorption coefficient of the QCL waveguide, β is the coupling ratio of the spontaneous emission to the laser mode, and τ_{sp} is the lifetime of the spontaneous emission. For simplicity, we ignore the spontaneous emission term, assuming this value to be sufficiently small, and solve the above three expressions under an assumed steady state. The difference between the number of carriers in the upper and lower states of the laser, Δn, can then be expressed as in the following expression.

$$\Delta n = n_3 - n_2 = \frac{J}{e}\tau_3\left(1 - \frac{\tau_2}{\tau_{32}}\right) - n_2^{therm} \quad (4)$$

Here, we assume the relationship $n_2^{therm} = n_2 \exp(-\Delta/kT)$, which expresses the density of the carriers in state g that become distributed to state 2 due to thermal effects. In the case of a population inversion, $\Delta n > 0$ holds. If we assume $\Delta \gg kT$, $n_2^{therm} \ll n_2$ holds, the population inversion condition is then expressed as follows.

$$\tau_{32} > \tau_2 \quad (5)$$

For the above population inversion condition to be satisfied, the QCL places another state (1) below the lower state (2) of the laser. Making the energy difference, ΔE_{21}, between these two states slightly larger than the energy (E_{LO}) of the longitudinal optical (LO) phonon results in a short τ_2 using LO phonon scattering. The E – k dispersion curve of LO phonon scattering features only a small value of k dependence, and we can assume $E = E_{LO}$. For this reason, if the energy difference exceeds E_{LO}, LO phonon scattering becomes dominant. On the other hand, the upper state of the laser is smaller than E_{LO}, meaning that the laser in the upper state is not effective as a scattering mechanism. Consequently, the scattering time generally becomes longer and Expression (5) is satisfied.

2.2 Problems in laser oscillation in the terahertz (THz) band and techniques to resolve them

While the performance of QCLs is improving in the MIR range, when the emission frequency is in the THz range, the characteristics below, which do not arise in the MIR range, become conspicuous and render laser oscillation difficult.

(1) Significant waveguide loss

Various factors lead to light loss in a laser waveguide, including absorption loss, scattering loss, and mirror loss. Among these factors, absorption loss occurs due to absorption by the carriers in the waveguide (free carrier absorption). The magnitude of free carrier absorption can be obtained from the dielectric constant. If we assume the Drude model for a doped semiconductor, the dielectric constant e is expressed as in the following expression.

$$\varepsilon = (n + ik)^2 = 1 - \frac{\omega_p^2}{\omega^2 + i\gamma\omega} \quad (6)$$

Here, ω_p is the plasma frequency, γ is the damping factor, n is the real component of the complex refractive index, and k is the imaginary component of the complex refractive index. From this expression, we can derive the absorbance, α, of free carrier absorption as follows.

$$\alpha = \frac{4\pi k}{\lambda} \propto \lambda^{-2} \quad (7)$$

As shown in the expression, the magnitude of the absorbance is inversely proportional to the square of the wavelength, λ. The wavelength of THz waves (λ: approximately several hundred μm) is approximately ten times larger than that of MIR waves. Due to this wavelength dependence, absorption loss becomes conspicuous in the THz range if the same waveguide structure is used, though this phenomenon is not a problem in the MIR range. Accordingly, doping concentration control in

the active layer becomes difficult, and the waveguide structure itself requires improvements.

(2) Low carrier injection efficiency

In terms of energy, THz waves are in a range from several to several tens of meV. The energy difference between the upper and lower states of the laser is thus correspondingly small. As a result, the energy widths of the quantized states are close to the emission energy, which makes it difficult to inject the carriers selectively to the upper state of the laser from the carrier injection region. (Tunnel leakage to the lower state of the laser and other states increases.) Thus, it becomes difficult to produce the population inversion required to acquire sufficient gain, and the design of the injection barrier layer that will control this population inversion becomes important.

(3) Change in dominant carrier relaxation mechanisms

In the MIR-QCL, LO phonon scattering is the dominant carrier relaxation mechanism (without light emission). This is because the emission energy is larger than E_{LO} (36 meV for GaAs), and this property is used to produce the population inversion. On the other hand, the emission energy is smaller than E_{LO} in the THz-QCL, such that LO phonon scattering is not an effective mechanism. In this range, electron-electron scattering due to carrier injection and interface roughness scattering due to imperfections in the interface between different materials cannot be ignored. These features also pose difficulties in the design of the QC structure.

Despite these difficulties, certain groups have devised unique techniques leading to successful THz-QCL oscillation. Figure 5 shows schematic diagrams of the energy band profiles for typical active layer structures[11]-[13]. Figure 5 (a) shows the structure with the first successful THz-QCL; this is known as the chirped superlattice structure. This structure gradually changes the thickness of the quantum well (QW) and the barrier layers so that the minibands of the superlattice form flat bands when an operating electric field is imposed. The radiative transition occurs between the minibands. A carrier that has transitioned from the bottom of the upper miniband to the top of the lower miniband moves to the bottom of the miniband through a fast intra-miniband relaxation

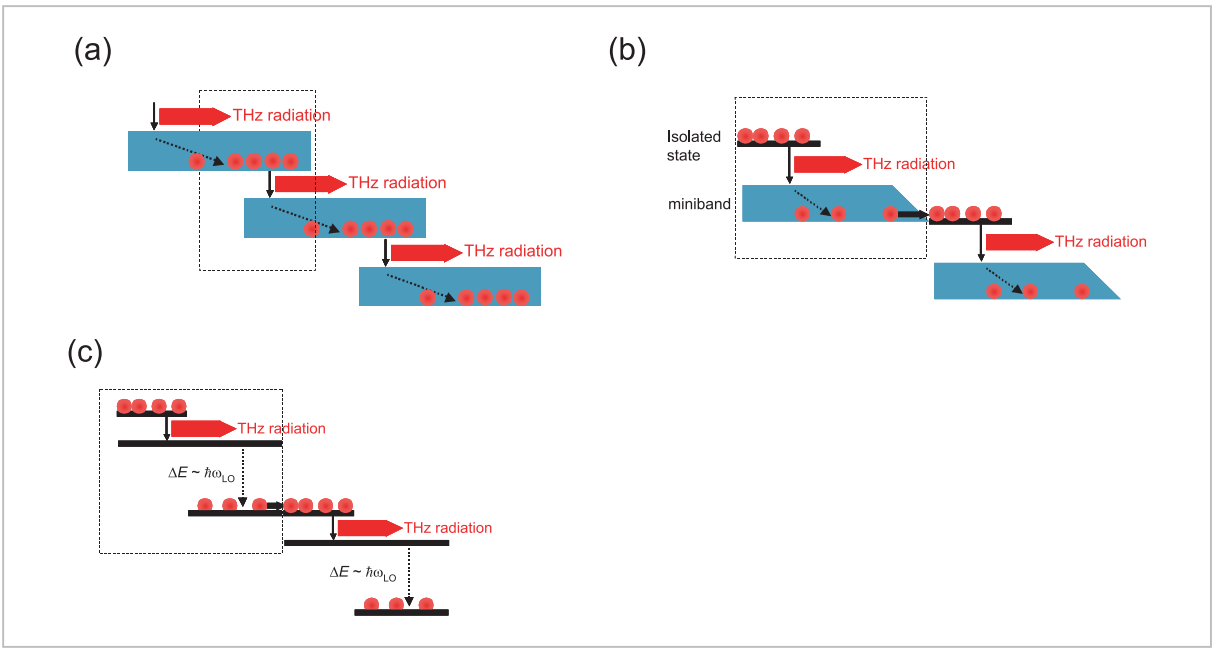

Fig.5 *Schematic diagrams of functions of energy band profiles of the well-known THz-QCL*

(a) chirped superlattice structure, (b) bound-to-continuum structure, and (c) resonant LO phonon extraction structure

process and is injected into the upper miniband of the next stage. Figure 5 (b) shows the structure known as the bound-to-continuum structure. As with the chirped superlattice structure, the bound-to-continuum structure uses intra-miniband relaxation for the extraction of the carriers in the lower state; the difference lies in that for the bound-to-continuum structure, the upper state of the laser is an isolated state instead of a miniband. Isolating the upper state increases the efficiency of carrier injection from the previous stage. Figure 5 (c) shows the structure known as the resonant LO phonon extraction structure; this is the structure we use in the description in section **2.1**. While the other two structures use intra-miniband relaxation for carrier extraction, the resonant LO phonon extraction structure uses LO phonon scattering. As stated earlier, LO phonon scattering is a fast relaxation phenomenon, offering corresponding advantages in reducing the carrier lifetime of the lower state. However, as the difference between the upper state of the laser and the carrier extraction state is also close to E_{LO} in the THz-QCL, the carrier lifetime of the upper state also becomes short in this device, and without corrective measures, population inversion cannot be produced. This structure avoids this problem by spatially moving the carrier that has transitioned to the lower state of the laser to the extraction/injection region by resonant tunneling, and then relaxing the carrier by LO phonon scattering. This mechanism can reduce the overlap between the wave functions of the upper state of the laser and the extraction state, which reduces the probability of LO phonon scattering and produces the population inversion.

On the other hand, new waveguide structures have also been proposed that take advantage of the long wavelength of THz waves. Figure 6 shows the two main waveguide structures currently employed[14]. In the electrode metal used for the laser element and the highly doped semiconductor material used for the contact layer, the second term in Expression (6) is larger than 1 for THz waves (due to the relationship, $\omega_p > \omega$), and the real component of the dielectric constant is negative. This means that the refractive index is imaginary. Thus, when THz waves enter this material, they attenuate significantly, and at the same time, generate the confinement mode (i.e., interface plasmon) at the interface. The waveguide of the THz-QCL makes use of this plasmon mode. Figure 6 (a) shows the semi-insulating surface plasmon (SISP) waveguide. The active layer confines light between the electrode metal of the upper face and the highly doped thin film of the lower face. In this case, the plasmon mode generated in the highly doped thin film extends to the substrate. To avoid absorption by the substrate, this structure uses a semi-insulating substrate. Figure 6 (b) shows the waveguide structure

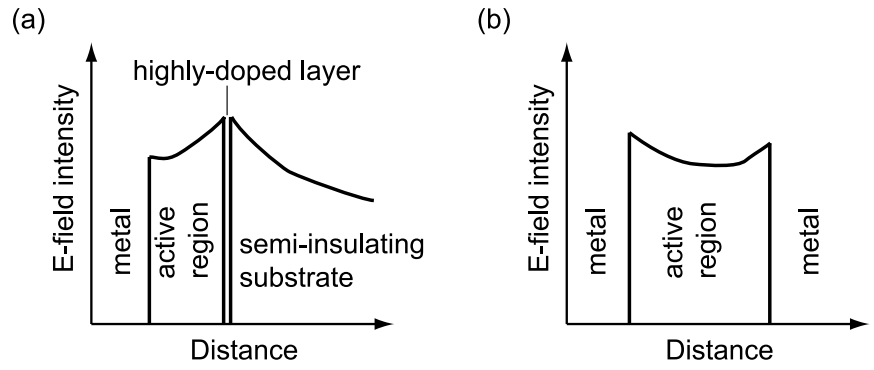

Fig.6 *Waveguide structures used in THz-QCL and mode profiles of light electric field confined by waveguides*

(a) SISP (semi-insulating surface plasmon) waveguide structure, (b) metal-metal (MM) waveguide structure

known as the metal-metal (MM) waveguide. Both the upper and lower faces are electrode metal, sandwiching the active layer. In this case, light does not propagate into the metal on both ends and is confined only in the active layer between the electrodes. Thus, this structure leads to a high confinement factor with a value of approximately 1.

2.3 Terahertz (THz) quantum cascade laser (THz-QCL)

Based on the characteristics discussed so far, this section describes the THz-QCL developed by our group. The laser structure is built on a semi-insulating GaAs substrate using the molecular beam epitaxy (MBE) method. The structure consists of 480 periods of GaAs/$Al_{0.15}Ga_{0.85}As$ resonant LO phonon extraction QC structures [Fig. 7 (a)] and Si-doped GaAs contact layers formed on the upper and lower faces. Figure 7 (b) shows a cross-sectional SEM image of the QCL structure grown, illustrating the formation of a periodical structure. For more detailed evaluation, we performed an X-ray diffraction evaluation and confirmed that the structure is formed within 2 % of the design value [Fig. 7 (c)]. We fabricated a Fabry-Perot

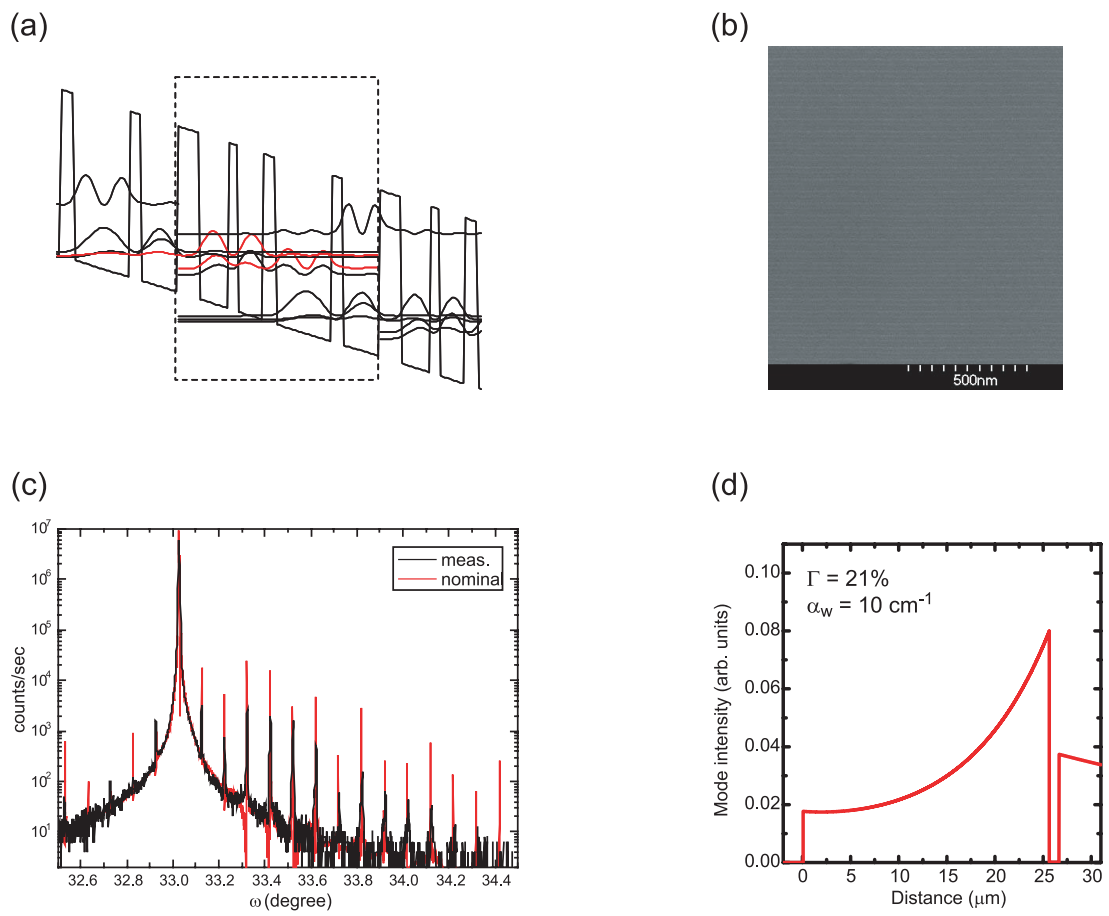

Fig.7 *Laser structure of THz-QCL*

(a) Active layer structure of developed THz-QCL. The film thickness of each layer enclosed in the dotted frame is as follows, from left to right: **5.4**/7.8/**2.4**/6.5/**3.8**/14.9/**3.0**/9.5. (The values are given in nm. Boldface values are for $Al_{0.15}Ga_{0.85}As$; remaining values are for GaAs. The underlined value indicates a Si-doped n-type semiconductor.) (b) Cross-sectional SEM image of THz-QCL. (c) X-ray diffraction spectrum of THz-QCL. (d) Mode profile of THz waves confined in the SISP waveguide. The confinement factor is $\Gamma = 21\,\%$ and the waveguide loss is $aw = 10\ cm^{-1}$.

waveguide with a mesa width of 200 μm and cavity length of 3 mm on this sample using the normal wet process. The laser facets used are a cleave facet for the output facet and a high-reflection film for the rear facet. The waveguide features a SISP waveguide structure, as shown in Fig. 7 (d).

Figure 8 shows the results of the evaluation of laser characteristics. Figure 8 (a) shows the current-voltage (I-V) characteristics and the current-light output (I-L) characteristics in a pulse-driven operation. The current pulse is 200 ns wide with a repetition frequency of 400 Hz. We performed measurement at the temperature of 39 K and measured the light output with a bolometric detector. As the figure shows, laser oscillation takes place with a threshold current density below 1 kA/cm^2. The peak output power is close to 30 mW. (A kink is observed in the IL characteristic, due to absorption by air in the measurement light path between the laser and the detector.) The threshold voltage is approximately 28 V, an extremely large value compared to the corresponding value for a semiconductor laser (approximately 1 V). This is characteristic of a QCL. Connecting many stages of QC structure units increases the entire voltage drop in accordance with the number of stages. The inserted figure shows the oscillation spectrum when the bias current is 5.1 A. As the figure illustrates, laser oscillation takes place at 3.1 THz. As indicated by the negative differential resistance (NDR) observed in the IV characteristics, output saturation is caused as the coupling between the states in the QC structure decouples and the designed carrier injection is no longer possible. Figure 8 (b) shows the temperature characteristics of the THz-QCL. The maximum operating temperature of this sample is 123 K. The characteristic temperature (T_0) exceeds 100 K, reaching 113 K directly before oscillation stops.

The example cited above uses a SISP waveguide structure. However, the MM waveguide is also an attractive waveguide structure, as the confinement factor is close to 1. Due to this large confinement factor, the figure of merit as defined by Γ/α is larger than that of the SISP waveguide structure, and a low threshold is expected. In addition, this characteristic enables narrow mesa width and short

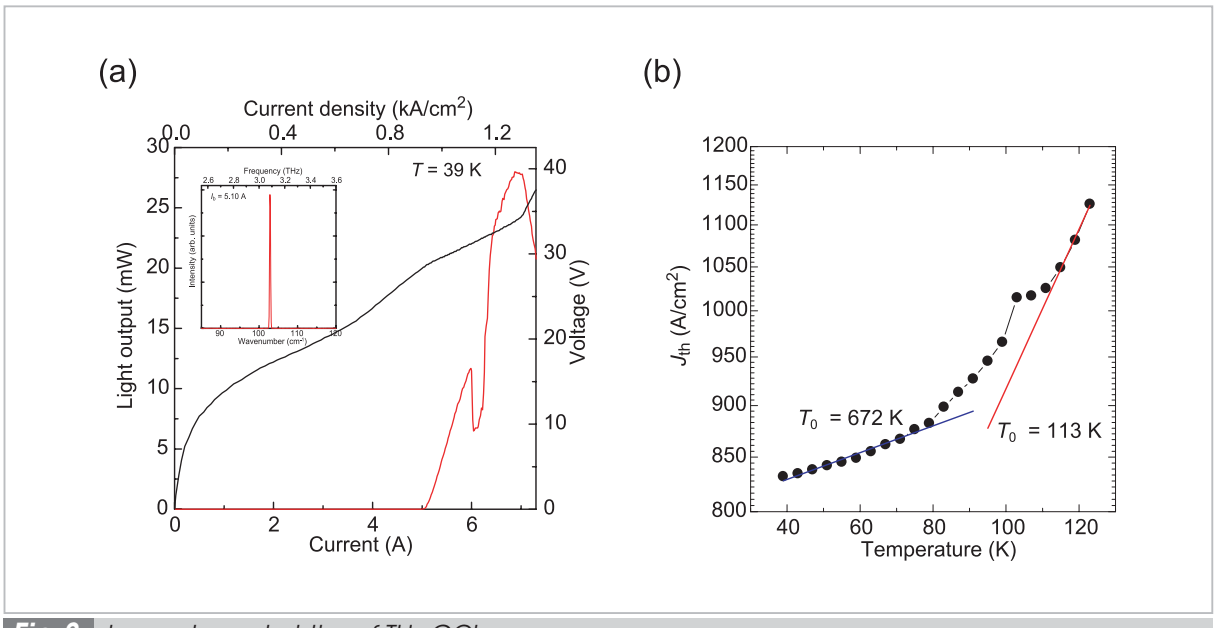

Fig.8 *Laser characteristics of THz-QCL*

(a) L-I-V characteristics. The sample features a threshold at approximately 5 A and produces output power close to 30 mW. The inserted figure shows the spectrum directly after laser oscillation. (b) Temperature dependence of threshold current density. Oscillation is confirmed up to 123 K. The characteristic temperature (T_0) is 113 K directly before oscillation stops.

cavity length, which is also advantageous in reducing power consumption. However, an MM waveguide presents a large impedance mismatch with the external load at the cavity facets in the THz range, reducing the light-extraction efficiency of the laser light. Thus, although this waveguide may be slightly disadvantageous in terms of increasing the output power of the THz-QCL, various techniques have been proposed to solve the problem[15]-[18]. In light of these considerations, our group also built an MM waveguide THz-QCL.

To fabricate the MM waveguide structure, we deposited gold (Au) on the surfaces of both the n-GaAs substrate and the THz-QCL epitaxial wafer, which was prepared using the crystal growth method, based on the MBE method (as in the case of the SISP waveguide). We then bonded the two components on the Au faces by thermocompression. In-Au bonding is widely used in the bonding of THz-QCL[19]. However, we selected Au-Au bonding for simplicity in handling. After bonding, we removed the substrate on the epitaxial side and fabricated the mesa structure using a wet process. Figure 9 (a) shows a cross-sectional SEM image of the fabricated mesa structure. As indicated by the inserted enlarged image, the bonding interface is well fabricated, without voids. Using this bonding technique, we fabricated a laser structure with a mesa width of approximately 100 μm and cavity length of approximately 2 mm and measured the light output-current-voltage characteristics. We succeeded in laser oscillation with a threshold current density of 0.3 kA/cm^2 at T = 15 K [Fig. 9 (b)]. We also succeeded in reducing the power consumption to approximately 1/20 relative to the THz-QCL, based on a SISP structure.

3 Conclusions

This article discussed the quantum cascade laser (QCL), a compact semiconductor light source. The THz-QCL device remains under development worldwide, with promising prospects for future development. When applications are considered, the THz-QCL will preferably produce output power of several tens of mW in a temperature range that can be achieved by electronic cooling techniques, such as cooling by a Peltiert device. Whether high-temperature and high-power characteristics can be achieved by a simple QC structure or whether a structure different from the QCL is required, optimism is high for future development.

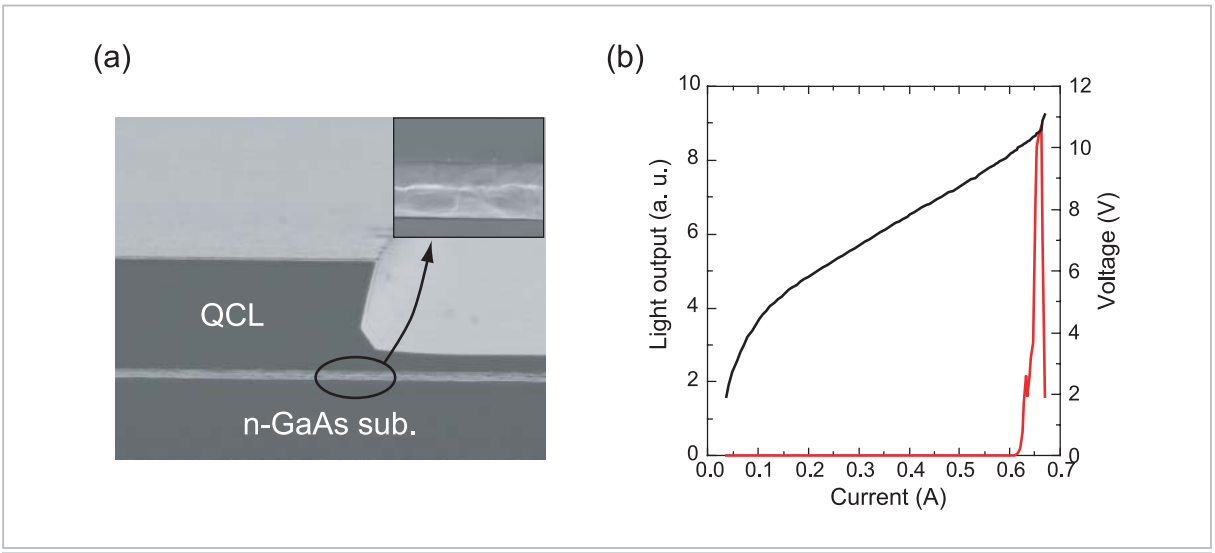

Fig.9 *(a) Cross-sectional SEM image of metal waveguide structure. The inserted figure shows the enlarged image of the bonding interface. (b) LIV characteristics of THz-QCL with MM waveguide structure.*

Acknowledgements

In this research undertaking we used the photonic device laboratory of the Koganei Headquarters for processing and related activities. We would like to thank Distinguished Researcher Itabe and the laboratory staff. We would also like to thank Professor Hirakawa of the Institute of Industrial Science, the University of Tokyo, who helped us in sample evaluation and related activities.

References

1 R. F. Kazarinov and R. A. Suris, Sov. Phys. 5, 707, 1971.
2 H. C. Liu, J. Appl. Phys. 63, 2856, 1988.
3 Q. Hu and S. Feng, Appl. Phys. Lett. 59, 2923, 1991.
4 A. Kastalsky, V. J. Goldman, and J. H. Abeles, Appl. Phys. Lett. 59, 2636, 1991.
5 J. P. Loehr, J. Singh, R. K. Manis, and G. I. Haddad, Appl. Phys. Lett. 59, 2070, 1991.
6 S. I. Borenstain and J. Katz, Appl. Phys. Lett. 55, 654, 1989.
7 J. -W. Choe, A. G. U. Perera, M. H. Francombe, and D. D. Coon, Appl. Phys. Lett. 59, 54, 1991.
8 Y. J. Mii, K. L. Wang, R. P. G. Karunasiri, and P. F. Yuh, Appl. Phys. Lett. 56, 1046, 1990.
9 G. N. Henderson, L. C. West, T. K. Gaylord, C. W. Roberts, E. N. Glytsis, and M. T. Asom, Appl. Phys. Lett. 62, 1432, 1993.
10 J. Faist, F. Capasso, D. L. Sivco, C. Sirtori, A. L. Hutchinson, and A. Y. Cho, Science 264, 553, 1994.
11 R. Köhler, A. Tredicucci, F. Beltram, H. Beere, E. Linfield, A. Davies, D. Ritchie, R. Lotti, and F. Rossi, Nature 417, 156, 2002.
12 G. Scalari, L. Ajili, J. Faist, H. Beere, E. Linfield, D. Ritchie, and G, Davies, Appl. Phys. Lett. 82, 3165, 2003.
13 B. Williams, H. Callebaut, S. Kumar, and Q. Hu, Appl. Phys. Lett. 82, 1015, 2003.
14 B. S. Williams, S. Kumar, H. Callebaut, Q. Hu, and J. L. Reno, Appl. Phys. Lett. 83, 5142, 2003.
15 O. Demichel, L. Mahler, T. Losco, C. Mauro, R. Green, J. Xu, A. Tredicucci, and F. Beltram, Opt. Express 14, 5335, 2006.
16 S. Kumar, B. S. Williams, Q. Qin, A. W. M. Lee, Q. Hu, and J. L. Reno, Opt. Express 15, 113, 2006.
17 M. I. Amanti, M. Fischer, C. Walther, G. Scalari, and J. Faist, Electron. Lett. 43, 573, 2007.
18 A. W. M. Lee, Q. Qin, S. Kumar, B. S. Williams, Q. Hu, and J. L. Reno, Opt. Lett. 32, 2840, 2007.
19 B. S. Williams, S. Kumar, H. Callebaut, Q. Hu, and J. L. Reno, Appl. Phys. Lett. 83, 2124, 2003.

***SEKINE Norihiko**, Ph.D.*

Senior Researcher, Advanced Communications Technology Group, New Generation Network Research Center

The Physical Properties of Semiconductor Nanostructures in the Terahertz Regime and Their Application to Terahertz Devices

***HOSAKO Iwao**, Ph.D.*

Research Manager, Advanced Communications Technology Group, New Generation Network Research Center

Terahertz Semiconductor Devices and Their Application to Measurement Systems